Available online at BCREC Website: http://bcrec.undip.ac.id

Bulletin of Chemical Reaction Engineering & Catalysis, 12 (3), 2017, 478-484

Research Article

Studying Impact of Different Precipitating Agents on Crystal Structure, Morphology, and Photocatalytic Activity of Bismuth Oxide

Yayuk Astuti[1]*, Arnelli[1], Pardoyo[1], Amilia Fauziyah[1], Siti Nurhayati[1], Arum Dista Wulansari[1], Rizka Andianingrum[1], Hendri Widiyandari[2], Gaurav A. Bhaduri[3]

[1]*Chemistry Department, Faculty of Science and Mathematics, Diponegoro University, Semarang, Central Java, Indonesia 50275*

[2]*Department of Physics, Faculty of Science and Mathematics, Diponegoro University, Semarang, Central Java, Indonesia 50275*

[3]*School of Chemical Engineering and Advanced Materials, Newcastle University, Newcastle upon Tyne, United Kingdom, NE1 7RU*

Received: 12nd April 2017; Revised: 24th June 2017; Accepted: 12nd July 2017; Available online: 27th October 2017; Published regularly: December 2017

Abstract

Bismuth oxide (Bi_2O_3) is a well-studied photocatalyst for degradation of various environmental contaminants. In this research Bi_2O_3 has been synthesized by precipitation method using two different bases (NH_4OH and NaOH). The samples thus obtained were then analyzed using FTIR, XRD, and SEM for surface functionalization, crystal structures and morphological differences, respectively. The Bi_2O_3 precipitated using NH_4OH showed a flower like structure made up of individual plates having α-Bi_2O_3 crystal structure. The precipitate obtained using NaOH showed a honeycomb like flower structure with a mixture of both *α*-Bi_2O_3 and *γ*-Bi_2O_3 crystal structure. Degradation of methyl orange (MO) was used as a model system to test the photocatalytic activity of the bismuth oxide. The Bi_2O_3 synthesized using NH_4OH showed superior photocatalytic degradation of methyl orange than the one synthesized using NaOH.

Keywords: Bismuth oxide; Photocatalyst; Precipitation; Precipitating agents

How to Cite: Astuti, Y., Arnelli, Pardoyo, Fauziyah, A., Nurhayati, S., Wulansari, A.D., Andianingrum, R., Widiyandari, H., Bhaduri, G.A. (2017). Studying Impact of Different Precipitating Agents on Crystal Structure, Morphology and Photocatalytic Activity of Bismuth Oxide. *Bulletin of Chemical Reaction Engineering & Catalysis*, 12 (3): 478-484 (doi:10.9767/bcrec.12.3.1144.478-484)

Permalink/DOI: https://doi.org/10.9767/bcrec.12.3.1144.478-484

1. Introduction

Bismuth oxide (Bi_2O_3) is a yellow colored crystal with a melting point of 817 °C and the boiling point of 1890 °C and insoluble in water. This material has six crystallographic polymorphs, i.e. a-Bi_2O_3, b-Bi_2O_3, g-Bi_2O_3, d-Bi_2O_3, e-Bi_2O_3, and w-Bi_2O_3 [1,2]. The excellent optical and electrical properties like high refractive index, high dielectric permittivity and high oxygen conductivity make this material a suitable contender for various applications such as solid electrolyte fuel cells (SEFC) [3], lighting source [4], solid battery [5], photocatalyst [6], and gas sensor [7].

Chemical, structural and electrical properties of a material are dependent on its method of

* Corresponding Author.
E-mail: yayuk.astuti@live.undip.ac.id (Astuti, Y.)
Telp.: +62-24-7460058 Fax.: +62-24-76480675

synthesis [8,9]. In the case of supported oxide catalyst the deposition method also plays an important role in the performance of the catalyst. The deposition method determines whether the catalyst is uniformly distributed on the support or accumulation of the oxide takes place on the areas of the support [10,11,12]. Therefore, various methods have been reported for synthesis Bi_2O_3 that include hydrothermal [13], direct precipitation [14-19], microwave [6,20], solution combustion [21,22], and sol gel [1]. Of all these methods, described for the synthesis of Bi_2O_3 particles, the precipitation method is one of the least complex and energy efficient. Some of the most common substances used as the precipitating agents are hydroxide [14-16] and ammonia/ammonium salts [14,17,18].

Zhong *et al.* [17] studied the use of different ammonium salt precipitants on the formation of Bi_2O_3. They do not find any change in the structural properties of the Bi_2O_3 synthesized by changing the precipitant. Rather reported that the Bi_2O_3 synthesized using $NH_3{\cdot}H_2O$ showed best photocatalytic activity due to high surface area, pore volume and pore size. Therefore, in the current study we test to see if the two most commonly used precipitants (i.e. NH_4OH and NaOH) have an effect structural and photocatalytic properties of Bi_2O_3. Additionally we used bismuth oxy nitrate as a source of bismuth as compared to the commonly used bismuth nitrate [14-19]. The results suggested that the Bi_2O_3 synthesized using NH_4OH formed α-Bi_2O_3, whereas the one synthesized using NaOH formed a mixture of α-Bi_2O_3 and γ-Bi_2O_3. The photocatalytic properties of the Bi_2O_3 synthesized using NH_4OH showed better activity than the Bi_2O_3 synthesized using NaOH.

2. Materials and Methods

The materials used in this research were bismuth oxynitrate ($Bi_5O(OH)_9(NO_3)_4$), nitric acid (65 %), NH_4OH, and NaOH which were purchased from Merck. The solutions were prepared in distilled water.

2.1 Synthesis of bismuth oxide using precipitation method

Synthesis of bismuth oxide was undertaken by mixing 10 g $Bi_5O(OH)_9(NO_3)_4$ and 20 mL citric acid with stirring continuously (600 rpm). When the transparent solution was obtained, subsequently the weak base NH_4OH was added till the white turbid suspension with pH 9 was formed. The precipitate obtained was then filtered and washed using distilled water and dried in an oven at 110 °C for 24 hours. The white powder was then calcined in furnace at 600 °C for 1 hour. After calcination, a yellow powder was obtained and used for further characterization. This procedure was similar to the one followed in literature [14] with slight modifications. The above procedure was repeated for synthesis of bismuth oxide with different precipitating agent by replacing NH_4OH with NaOH. In addition, the equipment system for synthesis of bismuth oxide is presented in Figure 1.

2.2 Characterization of the samples

The raw material bismuth subnitrate and the yellow powder were characterized using XRD (XRD Bruker with 2θ ranging from 10° to 80° and CuKα radiation (β = 0.15418 nm) at 40 kV and 30 mA), FT-IR (Prestige 21 (Shimadzu) with the wavenumber 400-4000 cm^{-1}), and SEM (JEOL-JSM-G510LV) in order to identify

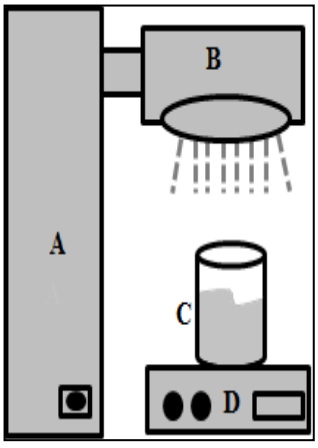

A : Lamp power supply
B : Solar lamp 1000 Wm^{-2}
C : Photocatalysis reactor
D : Hot plate magnetic stirrer

Figure 1. The equipment system for photocatalytic activity test

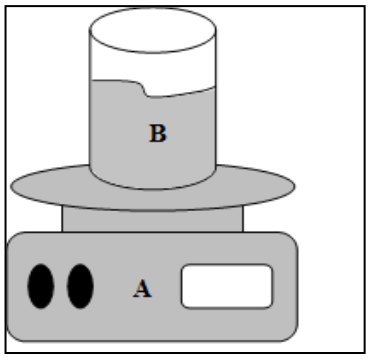

A : Hot plate magnetic stirrer
B : Synthesis reactor

Figure 2. The equipment system for synthesis of bismuth oxide

the crystal structure, the changing of functional groups, morphology and particle size, respectively.

2.3 Photocatalytic activity test

Photocatalytic activity of both Bi_2O_3 was tested using procedure reported previously [22]. 0.2 g bismuth oxide was added into 100 mL of 5 ppm methyl orange (MO). The mixture was irradiated using a solar simulator (PEC-L01, Peccell Technologies, Inc., Japan) as demonstrated in Figure 2 to simulate sunlight conditions with the powered density incident 1000 Wm^{-2}. In order for the dye to be completely adsorbed on the surface of catalyst prior to photocatalysis, the dye and catalyst solution was stirred in dark for 30 min. The photocatalysis experiment was carried out for 120 min under artificial solar irradiation and a sample was retrieved after every 20 min. The retrieved reaction mixture was then centrifuged at 6000 rpm for 5 min to separate the photocatalyst. The concentration of the supernatant was then measured using UV-Vis spectrophotometer at 463 nm.

3. Results and Discussion

The synthesis of Bi_2O_3 by precipitation method using NH_4OH and NaOH produced a white powder ($Bi(OH)_3$) after drying in the oven at 110 °C for 24 hours as seen in Figure 3a and 3b, respectively. After calcination at 600 °C for 1 h, the white powder changed its color to light yellow as seen in Figure 3c and 3d. The change in color indicated the formation of Bi_2O_3. As bismuth oxynitrate was used as a bismuth precursor as compared to previous reports that used bismuth nitrate [14-19], the reaction chemistry (with NH_4OH) is presented as follows:

$$Bi_5O(OH)_9(NO_3)_{4\,(s)} + HNO_{3\,(aq)} \rightarrow 5\,Bi(NO_3)_{3\,(aq)} + HNO_{3\,(aq)} + 10H_2O_{\,(l)}$$

$$Bi(NO_3)_{3\,(aq)} + 3NH_4OH_{\,(aq)} \rightarrow Bi(OH)_{3\,(s)} + 3NH_4NO_{3\,(aq)}$$

$$4\,Bi(OH)_{3\,(s)} \rightarrow 2\,Bi_2O_{3\,(s)} + 6\,H_2O$$

The XRD data for the synthesized Bi_2O_3 precipitate, using NH_4OH and NaOH, can be seen in Figure 4. When the Bi_2O_3 particles are synthesized using NH_4OH (Figure 4a), they seem to be in α-Bi_2O_3 phase. Iyyapushpam *et al.* [14] reported similar results, unfortunately no pH values were reported in their study. Later, Iyyapushpam *et al.* [15] reported the presence of γ-Bi_2O_3 using NH_4OH at pH 9.6

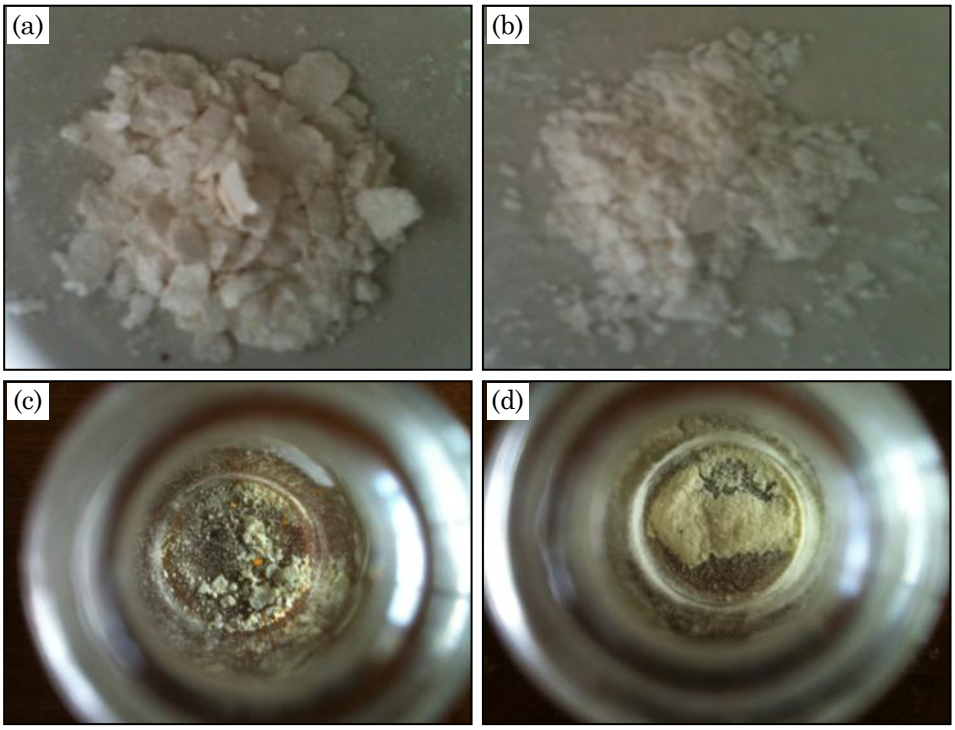

Figure 3. White product synthesized after heating the precipitate for 24 hours at 110 °C (a) using NH_4OH, and (b) using NaOH respectively. Pale yellow precipitate formed after calcination (c) of white powder formed using NH_4OH, and (d) of white powder formed using NaOH, respectively

and their study suggests that Bi_2O_3 synthesized at pH below 9.6 should be in γ-Bi_2O_3 phase. However, in this study the resultant reaction mixture pH was 9 and the phase of Bi_2O_3 obtained is α-Bi_2O_3. The calcination temperature used during the synthesis of Bi_2O_3 in the current study and by Iyyapushpam *et al.* [14] is higher than that used by Iyyapushpam *et al.* [15] which could be the reason for the formation of α-Bi_2O_3. It is known that α-Bi_2O_3 is a stable phase of bismuth oxide and other phases of Bi_2O_3 transform to the α-Bi_2O_3 phase under high temperature [19,23]. This indicates that both the resultant pH and the calcination temperature determine the phase of Bi_2O_3.

The XRD pattern for the Bi_2O_3 synthesized using NaOH is presented in Figure 4b. The phase of the Bi_2O_3 obtained using NaOH has a mixture of two phases. The most intensive peak 27.2° is close to the most intensive peak of both α-Bi_2O_3 and γ-Bi_2O_3 [19]. On comparing the diffraction patterns (a) and (b) in Figure 4, it can be seen that there are two additional peaks in pattern (b) (marked with asterisk) that correspond to γ-Bi_2O_3 [19]. This suggests that the material synthesized using NaOH is a mixture of both α-Bi_2O_3 and γ-Bi_2O_3, where α-Bi_2O_3 is the most dominant phase as seen from Figure 4b. Combining the results of this study with the previous study of Iyyapushpam *et al.* [14] suggests that during calcification the Bi_2O_3 first γ-Bi_2O_3 phase is formed and then it transforms into α-Bi_2O_3 phase. Therefore, the desired phase of Bi_2O_3 synthesized using precipitation method can be synthesized by regulating the calcification temperature alone.

FTIR spectra of Bi_2O_3 synthesized by precipitation method using NH_4OH and NaOH can be seen in Figure 5. The FTIR of the starting material (see Ref. [22]) shows sharp and intense vibration band at 1200-1700 cm^{-1} indicating the presence of nitrate (NO_3) and has been discussed previously [22]. Peaks observed between 3200-3600 cm^{-1} indicate the presence of OH groups [24,25]. The absence of dominant peaks between 1200-1700 cm^{-1} and 3200-3600 cm^{-1} in Figure 5 indicate the absence of both nitrate and hydroxide groups on the Bi_2O_3 surface. Moreover, the observed vibrational band between wavenumber 700-600 cm^{-1} and at ~830 cm^{-1} can be assigned to Bi–O–Bi vibration [24-27].

The SEM images of the Bi_2O_3 synthesized using NH_4OH show small plate like structures arranged in the flower like manner as seen in Figure 6a. It can be seen the flower like structure is made up of individual plate like structures having a thickness of ~20±10 nm. Duan *et al.* [28] synthesized similar flower like structures using bismuth oxide formate. Alternatively, the Bi_2O_3 synthesized using NaOH has a honeycomb like flower structure as presented in Figure 6b. Previously, Zhou *et al.* [9] synthesized similar flower like structure using VO_3^- as a precursor to get the desired shape of Bi_2O_3 particles. Comparing Figure 6a and 6b it can be seen that the sheets of Bi_2O_3 particles synthesized using NH_4OH are thicker than that of the particles synthesized using NaOH. As compared to the Figure 6a the particles in Figure 6b show a densely packed porous structure, having pore of 500-800 nm.

The photocatalytic activity of the synthesized Bi_2O_3 particles was evaluated by studying the degradation of aqueous solution of methyl orange under artificial solar irradia-

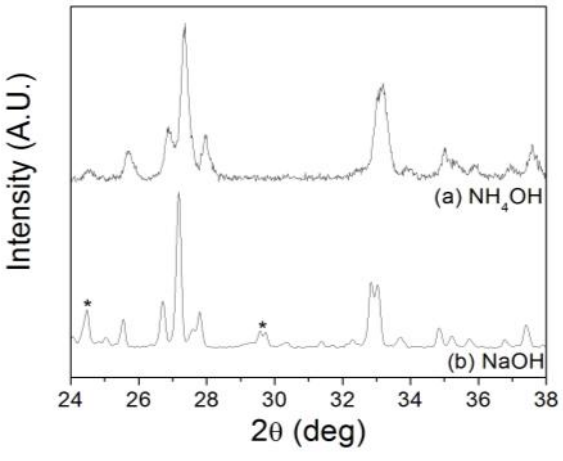

Figure 4. X-ray diffraction of bismuth oxide synthesized using (a) NH_4OH and (b) NaOH precipitating agents, respectively

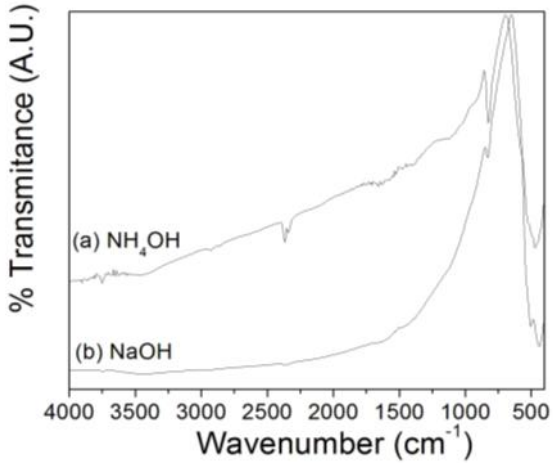

Figure 5. FTIR spectra of the Bi_2O_3 synthesized using (a) NH_4OH and (b) NaOH, respectively

tion. Figure 7a shows the photodegradation efficiency of methyl orange in absence and presence of the two flower like Bi_2O_3 synthesized using NaOH and NH_4OH, respectively, as a function of irradiation time. It can be seen that there was ~64 % degradation of methyl orange in the presence of Bi_2O_3 synthesized using NaOH as compared to ~78 % degradation of methyl orange in presence of Bi_2O_3 synthesized using NH_4OH in 120 min.

The kinetic evaluation of the photocatalyst was carried out by using the Langmuir-Hinshelwood model, for pseudo-first order kinetics given by the Equation (1) [14,15,29].

$$-ln\frac{C}{C_0} = kt \qquad (1)$$

where, C_o is the initial concentration of methyl orange, C is the concentration of methyl orange at different irradiation time, k is the kinetic constant of the reaction, and t is the irradiation time. Figure 7b shows the linear plot of $-\ln(C/C_0)$ vs t for the two flower like Bi_2O_3 catalysts, respectively. It can be seen from the Figure 7b that the Bi_2O_3 synthesized using NH_4OH had a higher kinetic rate constant of 12.5×10^{-3} s^{-1} as compared to Bi_2O_3 synthesized using NaOH of 8.8×10^{-3} s^{-1}. The kinetic rate constant of the Bi_2O_3 synthesized using NH_4OH was greater than that previously reported by Iyyapushpam *et al.* [14]. The reasons for the lower activity of Bi_2O_3 synthesized using NaOH is the presence of the partial γ-Bi_2O_3 phase. It is known that the γ-Bi_2O_3 has lower activity (about one order of magnitude) than that of α-Bi_2O_3 [14,15]. The catalytic activity of the Bi_2O_3 synthesized using NaOH had a higher activity than that of pure γ-Bi_2O_3 of 3.3×10^{-4} s^{-1} [15] and 1.1×10^{-4} s^{-1} [6].

4. Conclusions

Synthesis of Bi_2O_3 using the precipitation method with different precipitating agents was studied. The use weak base (NH_4OH) for Bi_2O_3 precipitation resulted in formation of plate

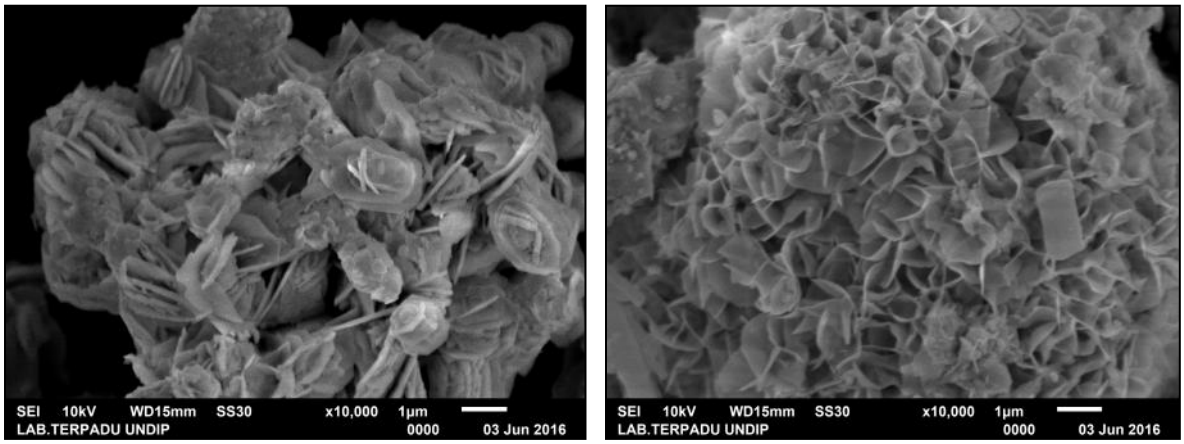

Figure 6. SEM images of bismuth oxide synthesized using (a) NH_4OH and (b) NaOH, respectively

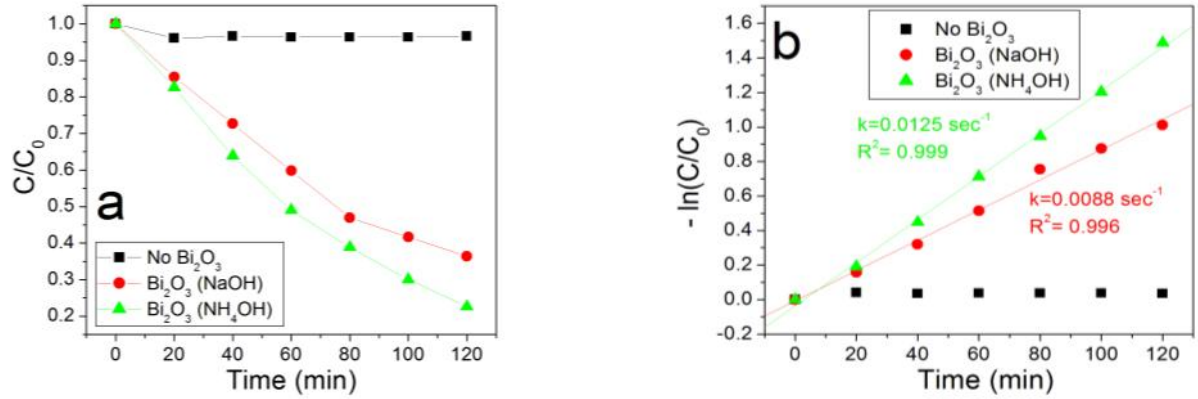

Figure 7. (a) Photodegradation of methyl orange in presence and absence of Bi_2O_3, and (b) kinetic linear simulation curves of the degradation of methyl orange in presence of Bi_2O_3 particles synthesized using NaOH and NH_4OH, respectively.

type structures arranged in the form of flowers. The use of strong base (NaOH) for precipitation of Bi_2O_3 led to formation of honeycomb like flower structure. Moreover, the photocatalytic activity of Bi_2O_3 synthesized using NH_4OH had better activity on degradation of methyl orange than the Bi_2O_3 synthesized using NaOH. The activity was dependent on the crystal structure of the Bi_2O_3.

Acknowledgement

The authors wish to acknowledge Faculty of Science and Mathematics, Diponegoro University for financial support with grant no. 3045/UN7.3.8/PG/2015, the Integrated Laboratory, Diponegoro University for XRD and SEM analysis and Laboratory of Organic Chemistry, Gajah Mada University for FTIR analysis.

References

[1] Mallahi, M., Shokuhfar, A., Vaezi, M.R., Esmaeilirad, A., Mazinani, V. (2014). Synthesis and Characterization of Bismuth Oxide Nanoparticles via Sol-Gel Method. *American Journal of Engineering Research*, 03: 162-165.

[2] Gomez, C.L., Depablos-Rivera, O., Silva-Bermudez, P., Muhl, S., Zeinert, A., Lejeune, M., Charvet, S., Barroy, P., Camps, E., Rodil, S.E. (2015). Opto-electronic Properties of Bismuth Oxide Films Presenting Different Crystallographic Phases. *Thin Solid Films,* 578: 103-112.

[3] Lee, J.G., Kim, S.H., Yoon, H.H. (2011). Synthesis of Yttria-Doped Bismuth Oxide Powder by Carbonate Coprecipitation for IT-SOFC Electrolyte. *Journal of Nanoscience and Nanotechnology,* 11(1): 820-823.

[4] Chu, Y.-C., Lee, G.J., Chen, C.Y., Ma, S.H., Wu, J.J., Horng, T.L., Chen, K.H. and Chen, J.H. (2013). Preparation of Bismuth Oxide Photocatalyst and Its Application in White-light LEDs. *Journal of Nanomaterials*, 2013: 1-7.

[5] Li, Y., Trujillo, M.A., Fu, E., Patterson, B., Fei, L., Xu, Y., Deng, S., Smirnov, S., Luo, H. (2013). Bismuth Oxide: A New Lithium-Ion Battery Anode. *Journal of Materials Chemistry A*, 1(39): 12123-12127.

[6] Liu, X., Pan, L., Lv, T., Sun, Z., Sun, C.Q. (2013). Visible Light Photocatalytic Degradation of Dyes by Bismuth Oxide-Reduced Graphene Oxide Composites Prepared via Microwave-Assisted Method. *Journal of Colloid and Interface Science*, 408: 145-150.

[7] Martirosyan, K.S., Wang, L., Vicent, A., Luss D. (2009). Synthesis and Performance of Bismuth Trioxide Nanoparticles for High Energy Gas Generator Use. *Nanotechnology,* 20(40): 1-8.

[8] Gotić, M., Popović, S., Musić, S. (2007). Influence of Synthesis Procedure on the Morphology of Bismuth Oxide Particles. *Materials Letters*, 61(3): 709-714.

[9] Zhou, L., Wang, W., Xu, H., Sun, S., Shang, M. (2009). Bi_2O_3 Hierarchical Nanostructures: Controllable Synthesis, Growth Mechanism, and their Application in Photocatalysis. *Chemistry - A European Journal*, 15(7): 1776-1782.

[10] Rubel, M.H.K., Miura, A., Takei, T., Kumada, N., Ali, M.M., Nagao, M., Watauchi, S., Tanaka, I., Oka, K., Azuma, M. (2014). Superconducting Double Perovskite Bismuth Oxide Prepared by a Low-Temperature Hydrothermal Reaction. *Angewandte Chemie International Edition*, 53(14): 3599-3603.

[11] Sarli, D.V., Landi, G., Lisi L., Saliva, A., Di Benedetto, A. (2016). Catalytic Diesel Particulate Filters with Highly Dispersed Ceria: Effect of the Soot-Catalyst Contact on the Regeneration Performance. *Applied Catalysis B: Environmental*, 197:116-124.

[12] Sarli, V.D., Landi, G., Lisi, L. (2017). Ceria-Coated Diesel Particulate Filters for Continuous Regeneration. *AlChE Journal,* AIChE Journal, 63(8): 3442-3449.

[13] Pérez, V.R., Bueno-López A. (2015). Catalytic Regeneration of Diesel Particulate Filters: Comparison of Pt and CePr Active Phases. *Chemical Engineering Journal,* 279: 79-85.

[14] Iyyapushpam, S., Nishanthi, S.T., Padiyan, D.P. (2013). Photocatalytic Degradation of Methyl Orange Using α-Bi_2O_3 Prepared without Surfactant. *Journal of Alloys and Compounds*, 563: 104-107.

[15] Iyyapushpam, S., Nishanthi, S.T., Padiyan, D.P. (2014). Enhanced Photocatalytic Degradation of Methyl Orange by Gamma Bi_2O_3 and Its Kinetics. *Journal of Alloys and Compounds*, 601: 85-87.

[16] López-Salinas, F.I., Martínez-Castañón, G.A., Martínez-Mendoza, J.R., Facundo Ruiz. (2010). Synthesis and Characterization of Nanostructured Powders of Bi_2O_3, BiOCl and Bi. *Materials Letters,* 64(14): 1555-1558.

[17] Zhong, J.B., Zeng, J., Li, J.Z., Hu, W. (2011). Photocatalytic Activity of Bi_2O_3 Prepared by Different Precipitants. *Advanced Materials Research*, 239-242: 998-1001.

[18] Lu, Y., He, X.Y., Zhong, J.B., Li, J.Z., Hu, W. (2012). Photocatalytic Activity of Bi_2O_3 Prepared by Different pH Value. *Advanced Materials Research*, 418-420: 554-557.

[19] Tseng, T.-K., Choi, J., Jung, D-W., Davidson, M., Holloway, P.H. (2010). Three-Dimensional Self-Assembled Hierarchical Architectures of Gamma-Phase Flowerlike Bismuth Oxide. *ACS Applied Materials & Interfaces*, 2(4): 943-946.

[20] Bartonickova, E., Cihlar, J., Castkova, K. (2007). Microwave-assisted Synthesis of Bismuth Oxide. *Processing and Application of Ceramics*, 1(1-2): 29-33.

[21] La, J., Huang, Y., Luo G., Lai, J., Liu, C., Chu, G. (2013). Synthesis of Bismuth Oxide Nanoparticles by Solution Combustion Method. *Particulate Science and Technology*, 31(3): 287-290.

[22] Astuti, Y., Fauziyah, A., Nurhayati, S., Wulansari, A.D., Andianingrum, R., Hakim, A.R., Bhaduri, G. (2016). Synthesis of α-Bismuth Oxide Using Solution Combustion Method and Its Photocatalytic Properties. *IOP Conference Series: Materials Science and Engineering*, 107(1): 1-7.

[23] Mehring, M. (2007). From Molecules to Bismuth Oxide-Based Materials: Potential Homo- and Heterometallic Precursors and Model Compounds. *Coordination Chemistry Reviews*, 251(7-8): 974-1006.

[24] Hu, Y., Liu, N.-H., Lin, U.-L. (1998). Glass Formation and Glass Structure of the $BiO_{1.5}$-PbO-CuO System. *Journal of Materials Science*, 33(1): 229-234.

[25] Narang, S.N., Patel, N.D., Kartha, V.B. (1994). Infrared and Raman Spectral Studies and Normal Modes of α-Bi_2O_3. *Journal of Molecular Structure*, 327(2): 221-235.

[26] Iordanova, R., Dimitriev, Y., Dimitrov, V., Kassabov, S., Klissurski, D. (1996). Glass Formation and Structure in the V_2O_5-Bi_2O_3-Fe_2O_3 Glasses. *Journal of Non-Crystalline Solids*, 204(2): 141-150.

[27] Iordanova, R., Dimitrov, V., Dimitriev, Y., Klissurski, D. (1994). Glass Formation and Structure of Glasses in the V_2O_5-MoO_3-Bi_2O_3 System. *Journal of Non-Crystalline Solids*, 180(1): 58-65.

[28] Duan, F., Zheng, Y., Liu, L., Chen, M., Xie, Y. (2010). Synthesis and Photocatalytic Behaviour of 3D Flowerlike Bismuth Oxide Formate Architectures. *Materials Letters*, 64(14): 1566-1569.

[29] Yang, L.-L., Han, Q-F, Zhao, J., Zhu, J-W., Wang, X., Ma, W-H. (2014). Synthesis of Bi_2O_3 Architectures in DMF-H_2O Solution by Precipitation Method and their Photocatalytic Activity. *Journal of Alloys and Compounds*, 614: 353-359.